JYX
JYVÄSKYLÄN YLIOPISTO
UNIVERSITY OF JYVÄSKYLÄ

This is a self-archived version of an original article. This version may differ from the original in pagination and typographic details.

Author(s): Taponen, Anni; Wong, Joanne W. L.; Lekin, Kristina; Assoud, Abdeljalil; Robertson, Craig M.; Lahtinen, Manu; Clérac, Rodolphe; Tuononen, Heikki; Mailman, Aaron; Oakley, Richard T.

Title: Non-Innocent Base Properties of 3- and 4-Pyridyl-dithia- and Diselenadiazolyl Radicals : The Effect of N-Methylation

Year: 2018

Version: Accepted version (Final draft)

Copyright: © 2018 American Chemical Society

Rights: In Copyright

Rights url: http://rightsstatements.org/page/InC/1.0/?language=en

Please cite the original version:

Taponen, A., Wong, J. W. L., Lekin, K., Assoud, A., Robertson, C. M., Lahtinen, M., Clérac, R., Tuononen, H., Mailman, A., & Oakley, R. T. (2018). Non-Innocent Base Properties of 3- and 4-Pyridyl-dithia- and Diselenadiazolyl Radicals : The Effect of N-Methylation. Inorganic Chemistry, 57(21), 13901-13911. https://doi.org/10.1021/acs.inorgchem.8b02416

Non-Innocent Base Properties of 3- and 4-Pyridyl-Dithia- and Diselenadiazolyl Radicals; the Effect of *N*-Methylation

Anni I. Taponen,[†] Joanne W. L. Wong,[#] Kristina Lekin,[#] Abdeljalil Assoud,[#] Craig M. Robertson,[⊥] Manu Lahtinen,[†] Rodolphe Clérac,[∀,∠] Heikki M. Tuononen[†], Aaron Mailman,[†,#,] and Richard T. Oakley[#,*]*

Department of Chemistry, University of Jyväskylä, P.O. Box 35, Jyväskylä, Finland; Department of Chemistry, University of Waterloo, Waterloo, Ontario N2L 3G1, Canada; Department of Chemistry, University of Liverpool, Liverpool, L69 7ZD, United Kingdom; Université de Bordeaux, CRPP, UPR 8641, F-33600 Pessac, France.

[†] University of Jyväskylä.

[#] University of Waterloo.

[⊥] University of Liverpool.

[∀] CNRS.

[∠] Univ. Bordeaux.

Abstract

Condensation of persilylated nicotinimideamide and isonicotinimideamide with sulfur monochloride affords double salts of the 3-,4-pyridyl-subtituted 1,2,3,5-dithiadiazolylium DTDA cations of general formula [3-, 4-pyDTDA][Cl][HCl], in which the pyridyl nitrogen serves as a non-innocent base. Reduction of these salts with triphenylantimony followed by deprotonation of the intermediate protonated radical affords the free base radicals [3-, 4-pyDTDA], the crystal structures of which, along with those of their diselenadiazolyl analogues [3-, 4-pyDSDA], have been characterized by powder or single crystal X-ray diffraction. The crystal structures consist of "pancake" π-dimers linked head-to-tail into ribbon-like arrays by η^2-S_2---N(py) intermolecular secondary bonding interactions. Methylation of the persilylated (iso)nicotinimide-amides prior to condensation with sulfur monochloride leads to *N*-methylated double chloride salts Me[3-, 4-pyDTDA][Cl]$_2$, which can be converted by metathesis into the corresponding triflates Me[3-, 4-pyDTDA][OTf]$_2$ and then reduced to the *N*-methylated radical triflates Me[3-, 4-pyDTDA][OTf]. The crystal structures of both the *N*-methylated double triflate and radical triflate salts have been determined by single crystal X-ray diffraction. The latter consist of *trans*-cofacial π-dimers strongly ion-paired with triflate anions. Variable temperature magnetic susceptibility measurements on both the neutral and radical ion dimers indicate that they are diamagnetic over the temperature range 2-300 K.

Introduction

1,2,3,5-Dithiadiazolyl (DTDA) radicals have been widely studied for many years,[1] initially with a view to their utilization as building blocks for molecular magnetic materials,[2] molecular semiconductors and conductive charge transfer salts $[DTDA]^{\delta+}[X]^{\delta-}$.[3] More recently they have also been explored as ligands to *d*- and *f*-block metals,[4] fluorophores in solution and polymer composites,[5] external field-driven NLO switches,[6] and paramagnetic guests in porous[7] and non-porous host frameworks.[8] In the absence of steric protection, DTDA radicals associate in the solid state, forming nominally diamagnetic dimers which display a partial or complete loss of their $S = ½$ magnetic signature. Selenium-based (DSDA) analogues have also been investigated, and in these systems the tendency to dimerize is even stronger, although, as with DTDAs,[9] steric effects can impede dimerization.[10] Pairwise association of the radicals by overlap of their SOMOs can occur in a variety of ways, some of which are shown in Chart 1. Of these, by far the most common is the *cis*-cofacial mode, which involves the direct superposition of two radicals separated by a pair of 4-center 2-electron[11] S---S (or Se---Se)[12] contacts. The nature of these interactions, now commonly referred to as "pancake" π-bonds,[13] has been the subject of much debate, the focus being on whether the pairing of the singly occupied molecular orbitals (SOMOs) of two radicals affords an open- or closed-shell singlet state.

Chart 1

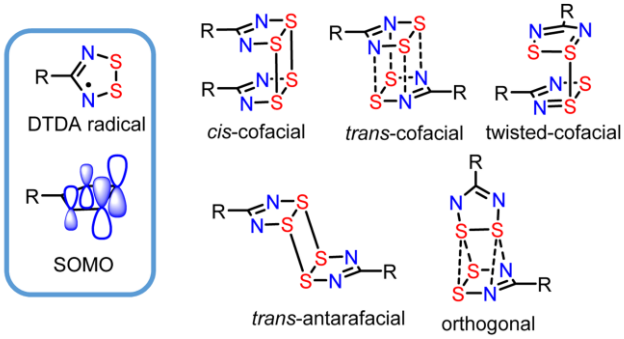

Considerable synthetic effort has been directed towards the control of the dimerization mode and packing pattern of the resulting pairs, partly with the intent of encouraging π-stacked dimer arrays, which historically were viewed as the most effective way to introduce a pathway for charge transport.[1c,3a,14] One approach that has served well has been the use of intermolecular secondary bonding interactions (SBIs) between the disulfide (diselenide) unit of the DTDA (DSDA) ring and a lone-pair carrying heteroatom attached to the 4-substituent. The effect was first demonstrated in the 2-, 3- and 4-cyanophenyl DTDA (DSDA) dimers,[15] and later extended to cyanofuryl[16] and cyanothienyl[17] derivatives. In all these materials the dimers are connected into ribbon-like arrays linked by η^2-S_2---NC SBIs (Figure 1). The resulting ribbons then pack into layers which, in some cases, afford the desired superimposed π-stack arrays, with the DSDA derivatives displaying small bandgap semiconductive properties.[14] From a magnetic perspective a vital modification of this strategy, developed by Rawson and coworkers in the mid-1900's, involved attachment of a cyano (or nitro) group to an otherwise fully fluorinated phenyl substituent on a DTDA radical.[18] The impact was two-fold: (i) the η^2-S_2---NC (or η^2-S_2---O_2N) SBIs locked the radicals into ribbons, and (ii) the steric protection afforded by perfluorination of the phenyl group suppressed dimerization. The discovery of these undimerized DTDA radicals and their sometimes startling magnetic properties[19] represents one of the major triumphs in the development of radical-based molecular materials.

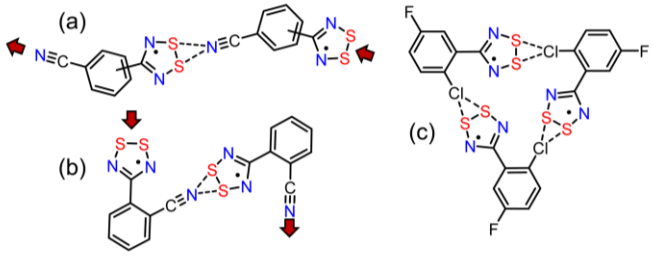

Figure 1. Ribbon-like arrays of radicals (dimers) linked by η^2-S_2···NC SBIs in (a) 3-, 4-cyanophenyl-DTDA and (b) 2-cyanophenyl-DTDA (ref. 15). (c) Triangular motif generated by η^2-S_2···Cl SBIs in 2-chloro-5-fluorophenyl-DTDA (ref. 20).

Exploration of ligand design and the resulting effect on solid state architecture continues, and the range of structure-making SBIs has been expanded. The packing of 2-chlorophenyl substituted DTDA dimers, for example, are dominated by short η^2-S_2---Cl intermolecular contacts which, like η^2-S_2---NC SBIs, are effective in generating layered structures.[20] Likewise the 2-pyridyl-substituted radicals 2-pyDTDA and 2-pyDSDA and related pyrimidyl derivatives developed by Preuss and coworkers serve as chelating (Chart 2) ligands to paramagnetic metal ions. The resulting coordination complexes display a rich array of magnetic properties, ranging from single molecule magnets to magnetically ordered materials and magnetothermal switches.[21] By contrast, the related 3-, 4-pyDTDA radicals[22] have received relatively little attention. A number of metal complexes have been reported,[23,24] but information on the radicals themselves is sparse, and the corresponding 3,4-pyDSDA derivatives are, to date, unknown. The relative dearth of information on these particular radicals may stem in part from the presence of a basic nitrogen on the ligand, which has caused some difficulties in their isolation. To address this issue we provide here full structural characterization of the dimers of the 3-, 4-pyDTDA and 3, 4-pyDSDA derivatives as well as modifications to the synthetic procedures made necessary by the "non-innocent" base properties of the pyridyl ligand. In addition, as a first step in taking advantage of

the coordination chemistry of the ligand, we also report the preparation and structural characterization of the *N*-methyl-pyridinium substituted radical salts Me[3-pyDTDA][OTf] and Me[4-pyDTDA][OTf].

Chart 2

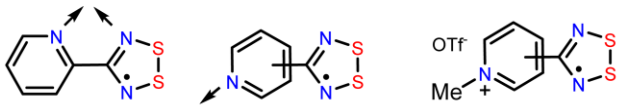

Results and Discussion

Synthesis. Early synthetic routes to the DTDA framework involving the addition reactions of thiazyl halides[25] or sulfur monochloride/ammonium chloride mixtures[26] to nitriles have been largely replaced by methods based on the condensation of an amidine, more particularly a persilylated amidine,[27] with sulfur monochloride or dichloride, to afford an oxidized dithiadiazolylium chloride salt. Reduction of the latter, typically with triphenylantimony, liberates the neutral radical, which may be purified by vacuum sublimation. This methodology, which is easily extended to the preparation of selenium-based analogues,[28] provides the basis for the synthesis of 3-, 4-pyDTDA and 3-, 4-pyDSDA described here.

The necessary persilylated amidines 3- and 4-pyADS were generated by the addition of lithium bis(trimethylsilylamide) to the appropriate nitrile (3-NCpy, 4-NCpy), followed by quenching the intermediate lithiated amidinate with chlorotrimethylsilane (Scheme 1A). Typically, such reactions employ diethyl ether or toluene/ether mixtures as the reaction solvent, but for these pyridyl-substituted nitriles the use of the more strongly basic solvent tetrahydrofuran is critical in order to suppress solvation of Li^+ ions with the pyridyl nitrogen and to keep the otherwise insoluble lithiated intermediate in solution. Consistently, the subsequent silylation step can only

be effected in tetrahydrofuran at reflux. The resulting persilylated amidines may then be purified by fractional distillation in vacuo.

Most silylated amidines undergo a smooth condensation with excess sulfur mono- or dichloride to afford directly the appropriate dithiadiazolylium chloride salt [DTDA][Cl] as an insoluble yellow-orange solid. However, for both 3- and 4-pyDTDA this general procedure requires modifications arising from the fact that the initial condensation reaction affords *not* the simple salt but its highly moisture-sensitive hydrochloride double salt, that is, [3, 4-pyDTDA][Cl][HCl], in which the pyridyl nitrogen is protonated (Scheme 1B). By contrast, protonated intermediates are not observed in the preparation of the analogous perfluorinated derivative 4-(F_4-py)-DTDA, as a result of the weaker base strength of the perfluoropyridyl moiety.[29] Reduction of these double salts with triphenylantimony in MeCN then affords the corresponding hydrochloride salts of the radical, that is, [3-, 4-pyDTDA][HCl]. Finally, rinsing these insoluble hydrochloride salts with a solution of excess triethylamine in MeCN liberates the free-base radicals 3-, 4-pyDTDA, which may be purified by fractional sublimation in vacuo. The sequence of events may be conveniently tracked by infrared spectroscopy, as illustrated in Figure 2 (see also Figure S1) which shows the spectral changes observed during the preparation of 4-pyDTDA.

Scheme 1

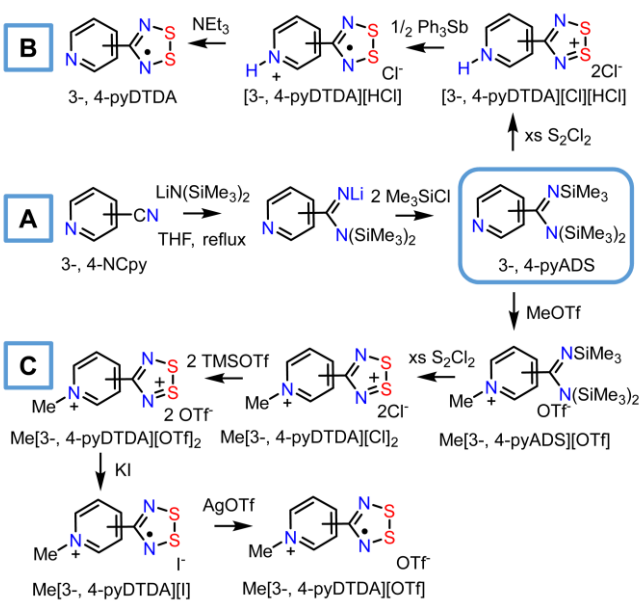

To explore more fully the stepwise nature of the synthesis of 3-, 4-DTDA, we pursued the *N*-methylated analogues of the protonated intermediates described above, with a view to obtaining structural information. To this end we prepared the *N*-methylated amidinium triflate salts Me[3-, 4-pyADS][OTf] by treatment of the respective persilylated amidine with methyl triflate (Scheme 1C). Condensation of these materials with sulfur monochloride afforded the double chloride salts Me[3-, 4-pyDTDA][Cl]$_2$, the methylated analogues of the protonated double salts described above. Metathesis of these chloride salts with trimethylsilyl triflate (TMSOTf) provided access to the corresponding double triflates Me[3-, 4-pyDTDA][OTf]$_2$, crystals of which were suitable for crystallographic work. Finally, reduction of these double salts with potassium iodide yielded the *N*-methyl radical iodides Me[3-, 4-pyDTDA][I] which, upon treatment with silver triflate, were converted into *N*-methyl radical triflates Me[3-, 4-pyDTDA][OTf], crystals of which were also suitable for crystallographic analysis.

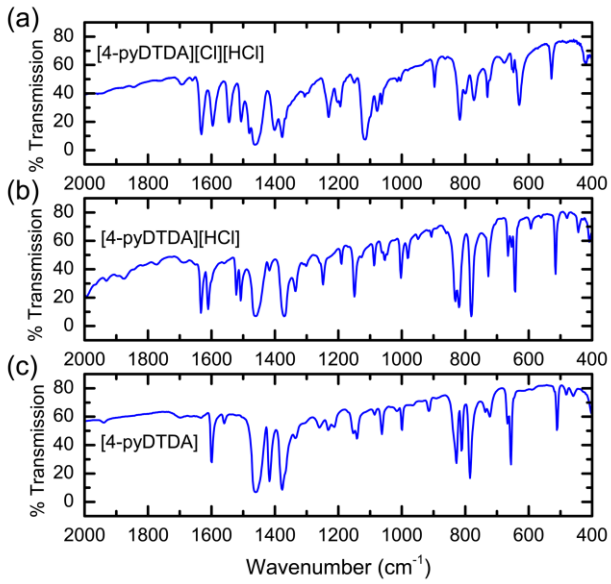

Figure 2. Infrared spectra (as nujol mulls) of intermediates in the synthesis of 4-pyDTDA, as shown in Scheme 1A: (a) [4-pyDTDA][Cl][HCl] double salt, (b) [4-pyDTDA][HCl] protonated radical salt and (c) neutral [4-pyDTDA].

Preparation of the selenium-based radicals 3-, 4-pyDSDA was more straightforward than that described above for 3-, 4-pyDTDA, possibly because the condensation reaction employed stoichiometric amounts of $SeCl_2$ generated by comproportionation of Se and $SeCl_4$,[28] as a result of which the presence of adventitious HCl (present in S_2Cl_2) was all but eliminated. Accordingly, the simple chlorides [3-, 4-pyDSDA][Cl] were generated directly during the condensation (Scheme 2), and reduction of these salts with triphenylantimony then released the corresponding radical dimers, which could be purified by sublimation in vacuo.

Scheme 2

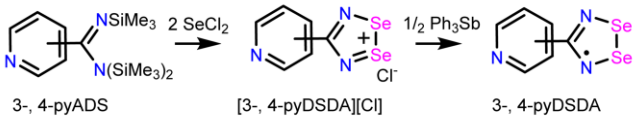

Crystallography on Radical Dimers. Analytically pure samples of the dimers of the four radicals 3-, 4-pyDTDA and 3-, 4-pyDSDA were generated by fractional sublimation in vacuo. Crystals of 3-pyDTDA and 3-, 4-pyDSDA so obtained were suitable for structural analysis by single crystal X-ray diffraction methods. Crystal data are summarized in Table S1 and ORTEP drawings of the dimer units are shown in Figure 3.

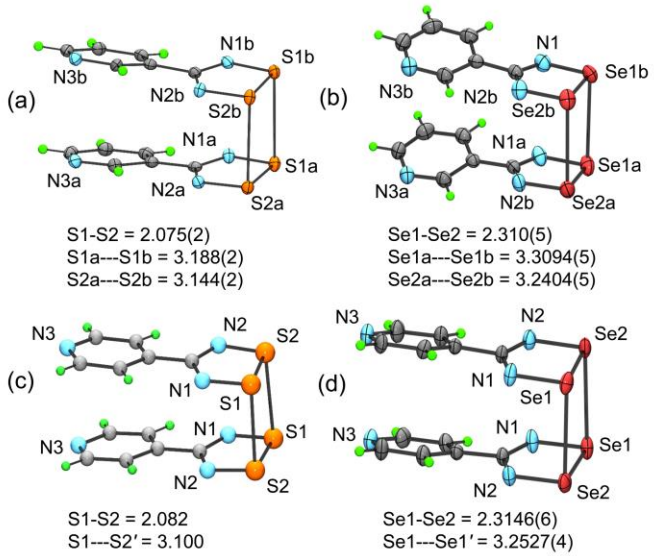

Figure 3. Drawings of dimer units in (a) 3-pyDTDA, (b) 3-pyDSDA, (c) 4-pyDTDA and (d) 4-pyDSDA, with atom numbering and selected metrics in Å; for averaged values, numbers in parentheses are the greater of the difference and the standard deviation. Thermal ellipsoids and standard deviations are not available for 4-pyDTDA.

The almost spherical, powdery nodules of 4-pyDTDA obtained by sublimation did not diffract as single crystals, but did generate a reproducible powder X-ray diffraction (PXRD) pattern consisting of a few sharp peaks and some broad "humps" (Figure 4), an appearance characteristic of a disordered nanocrystalline phase.[30] Material obtained by recrystallization from *o*-dichlorobenzene afforded a similar pattern. Changes in sample preparation, such as sample grinding, did not lead to a marked change in linewidth or resolution of the diffractogram.

Attempts to index the PXRD data collected on both laboratory and synchrotron X-ray sources with conventional indexing programs (DICVOL, McMaille, Topas) were unsuccessful, mainly because of the paucity and poor resolution of some of the diffraction peaks, which hindered assignment of a space group and specification of a unit cell. Eventually, however, by comparing the observed diffraction pattern with that predicted for the selenium analogue 4-pyDSDA we were able to index the data manually to the *C*2/*c* space group and identify a unit cell similar to that observed for both 4-pyDSDA and its perfluorinated variant 4-(F_4-py)DTDA.[29,31]

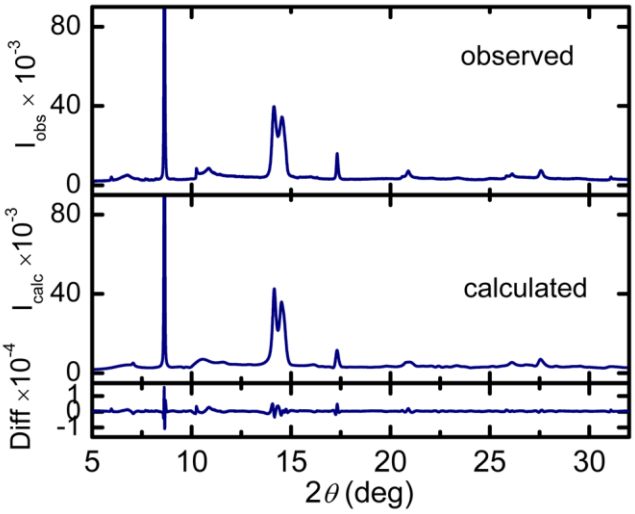

Figure 4. Observed and calculated PXRD pattern for *cis*-cofacial 4-pyDTDA (λ = 0.825925 Å).

The PXRD data was subsequently modelled in DASH using synthetic annealing methods based on a molecular unit adapted from the known molecular coordinates of 4-cyanophenyl-DTDA.[15] This procedure afforded a plausible solution based on *cis*-cofacial dimers (Figure 3c) linked head-to-tail into antiparallel chains in a fashion very similar to that found for 4-pyDSDA. This solution was refined by Rietveld methods using a rigid-body constraint in which only the unit cell parameters were optimized; the resulting crystal data are provided in Table S2 and the observed/calculated PXRD patterns are presented in Figure 4. Two other solutions with the same

cell parameters but based on *trans*-cofacial and *trans*-antarafacial dimers were similarly refined. The resulting (optimized) crystal data are provided in Table S2 and observed and calculated PXRD patterns are presented in Figures S2 and S3. The observation of these additional solutions is symptomatic of a disordered nanocrystalline phase[30] in which there is a large number of faults in the layering of the molecular ribbons.

The molecular metrics for 3-pyDTDA and 3,4-pyDSDA, notably the internal and intradimer S-S (Se-Se) distances are all nominal for this class of radicals. In the *cis*-cofacial dimer of 4-pyDTDA, positional refinements were not carried out, but the mean intradimer S-S separation (3.10 Å) is consistent with that observed in 4-cyanophenyl-DTDA (3.10(2) Å). The crystal packing of all four dimers follows the pattern observed for the related cyanophenyl derivatives, being comprised of ribbon-like arrays of *cis*-cofacial dimers linked head-to-tail by short η^2-S_2---N(py) and η^2-Se_2---N(py) SBIs; summaries of pertinent intermolecular metrics are provided in Figures S4 and S5. In the 3-pyDTDA and 3-pyDSDA (Figure 5), which are isostructural, the two radicals in the dimer unit are not related by symmetry, but in 4-pyDTDA and 4-pyDSDA (Figure 6) the two halves of the dimer are related by a 2-fold rotation. In all four cases the pyridyl group is rotated slightly about the connector C-C linkage, affording C-C-C-N torsion angles ranging from 8.1° in 4-pyDTDA to 16.8° in 4-pyDSDA. Packing patterns for the simulated annealing solutions based on *trans*-cofacial and *trans*-antarafacial 4-pyDTDA dimers are provided in Figures S6 and S7.

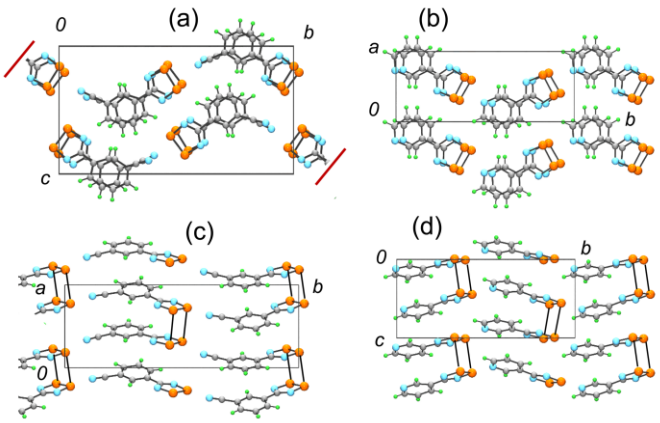

Figure 5. Antiparallel ribbon-like arrays of dimers in (a) α-3-cyanophenyl-DTDA ($P2_1/n$) and (b) 3-pyDTDA ($P2_1$) linked head-to-tail by η^2-S_2---NC and η^2-S_2---N(py) SBIs respectively. Out-of-register, superimposed π-stacks of dimers for each are shown in (c) and (d). The corresponding DSDA dimers are isostructural.

.

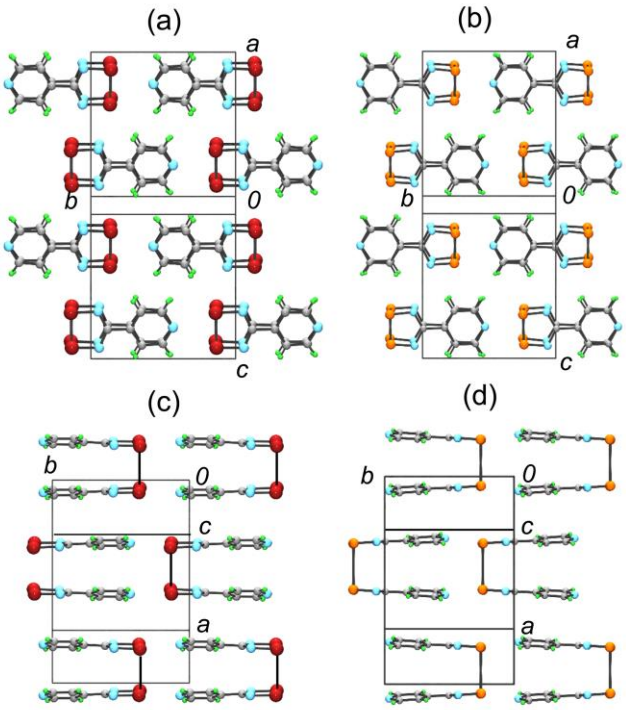

Figure 6. Antiparallel ribbon-like arrays of *cis*-cofacial dimers in (a) 4-pyDSDA and (b) 4-pyDTDA, linked head-to-tail by η^2-Se---N(py) and η^2-S_2---N(py) SBIs respectively, as viewed parallel to a^*. Head-over-tail stacking of π-dimers is shown in (c) and (d).

Crystallography on *N*-Methylated Salts

Crystals of the *N*-methylated double triflates Me[3-, 4-pyDTDA][OTf]$_2$ and radical ion triflates Me[3-, 4-pyDTDA][OTf] obtained by crystallization from MeCN were all suitable for structural characterization by single crystal X-ray diffraction. Crystal data for these materials are summarized in Table S3, and ORTEP drawings with intramolecular metrics are provided in Figures 7 and 8. At the molecular level, reduction of the double salts leads to a slight lengthening of the S-S and S-N bonds, in accord with the antibonding nature of the radical SOMO (Chart 1); similar effects are found in neutral DTDA structures. Strong ion pairing between the triflate anion(s) and the DTDA rings is observed in all four salts, and the *trans*-cofacial mode of dimerization found in the radical ion salts is probably driven by the need to facilitate a close electrostatic contact between the triflate anion and *N*-methyl pyridinium cation.

The steric bulk of the triflate anions restricts the extent of interdimer interactions in the radical ion salts. In Me[3-pyDTDA][OTf], space group $P\bar{1}$, the ion-paired dimers adopt a 1D head-over-tail slipped π-stack packing pattern running parallel to the *b*-axis, with no close interdimer contacts between the inversion-related dimers. In Me[4-pyDTDA][OTf], space group $P2_1/c$, the dimers are aligned into chains in which neighboring dimers are related by *c*-glides, an arrangement that produces a near orthogonal overlap.

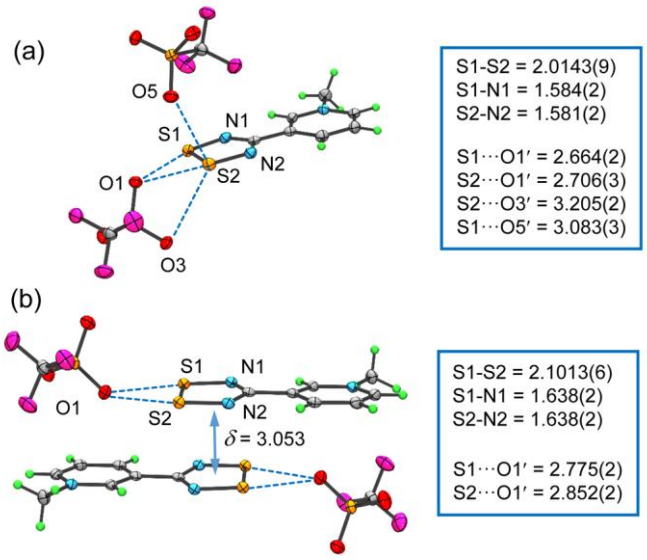

Figure 7. ORTEP drawings (50% ellipsoids) of (a) the asymmetric unit in Me[3-pyDTDA][OTf]$_2$ and (b) the *trans*-cofacial dimer in Me[3-pyDTDA][OTf], with selected bond distances and interionic contacts (dashed lines) in Å (all at 120 K). The $(CN_2S_2)_2$ interplanar separation δ (in Å) is also shown.

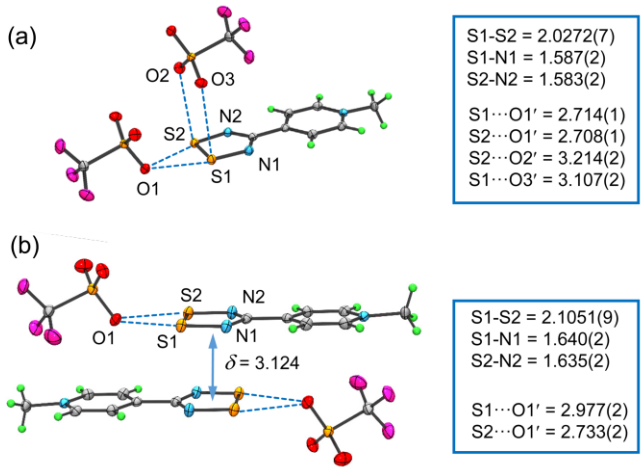

Figure 8. ORTEP drawings (50% ellipsoids) of (a) the asymmetric unit in Me[4-pyDTDA][OTf]$_2$ and (b) the *trans*-cofacial dimer in Me[4-pyDTDA][OTf], with selected bond distances and interionic contacts (dashed lines) in Å (all at 120 K). The $(CN_2S_2)_2$ interplanar separation δ (in Å) is also shown.

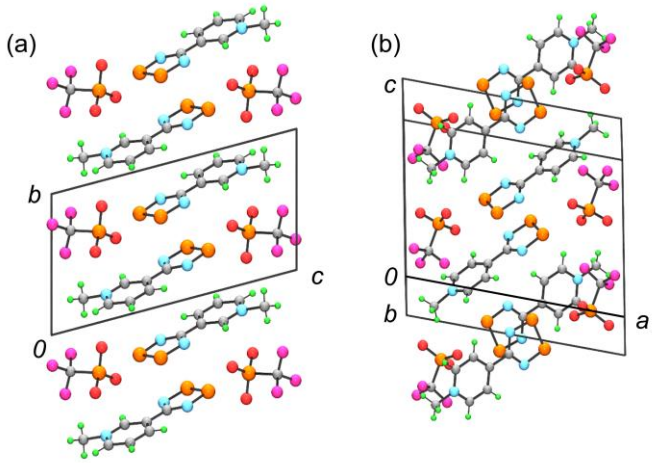

Figure 9. Unit cell drawings for (a) Me[3-pyDTDA][OTf], space group $P\bar{1}$ and (b) Me[4-pyDTDA][OTf], space group $P2_1/c$. In (a) dimers form head-over-tail π-stacks and in (b) neighboring dimers are related by *c*-glides, which produces a near orthogonal overlap.

EPR Spectroscopy The X-band EPR spectra (g = 2.0111) of the native radicals 3-, 4-pyDTDA, recorded at ambient temperature on samples dissolved in dichloromethane, display a characteristic quintet pattern (Figure 10) arising from hyperfine coupling to two pseudo-equivalent ^{14}N nuclei (I = 1); the resulting a_N values (near 0.51 mT) derived by spectral simulation are nominal for this class of radical. [xref28b,32] As expected, there is no observable hyperfine coupling with the pyridyl nitrogen nuclei, although such interactions may contribute to spectral line broadening. The spectra of the corresponding *N*-methylated cation radicals, obtained from samples of the salts dissolved in MeCN were almost identical in position and appearance, with g = 2.009 and $a_N \sim$ 0.50 mT, suggesting that alkylation of the pyridyl ligand induces very little leakage of spin density in the DTDA ring. Isotropic spectral data for the corresponding 3-, 4-pyDSDA radicals could not be measured because the low solubility and high dissociation constants of the respective dimers reduced the signal intensity of the radicals to below the detection limit.

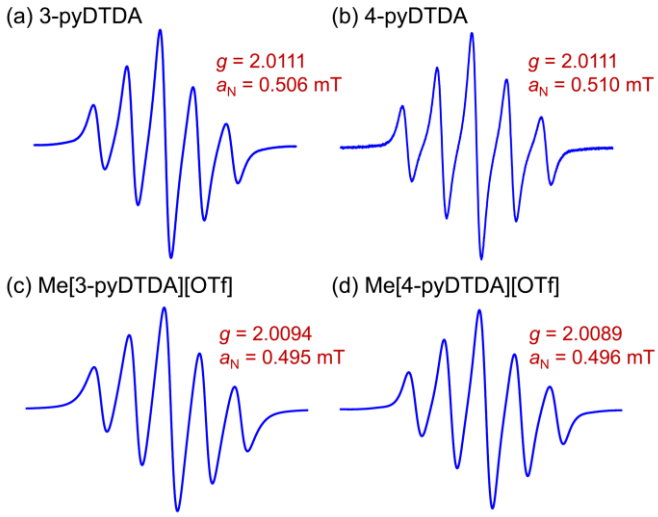

Figure 10. X-band EPR spectra (spectral width = 4 mT) of (a) 3-PyDTDA and (b) 4-pyDTDA in DCM, and of (c) Me[3-pyDTDA][OTf] and (d) Me[4-pyDTDA][OTf] in MeCN, all at 293 K.

Magnetic Measurements. Based on previous experience with other aryl-substituted DSDA dimers, which show little evidence of dissociation in the solid state below 300 K,[14] and the fact that neither of [3-, 4-pyDSDA] displays any EPR signal in the solid state, we have not explored their bulk magnetic properties. However, given that DTDA radicals often show complex magnetic behavior with temperature in the solid state, we have performed variable temperature magnetic susceptibility (χ) measurements on both the neutral radicals [3-, 4-pyDTDA] and their *N*-methylated salts Me[3-, 4-pyDTDA][OTf]. Data were collected in cooling mode using a static field *H* of 0.1 T over the range shown 2-300 K. As may be seen in Figure 11, the resulting plots of χ (corrected for diamagnetic contributions) versus *T* plots are remarkably similar. Both the neutral and charged radicals show essentially diamagnetic behavior, with a concentration of free spin defect impurities around the 1% level, which is as expected for DTDA dimers. There is no evidence for thermally induced dissociation up to 300 K, the limit of the experiment.

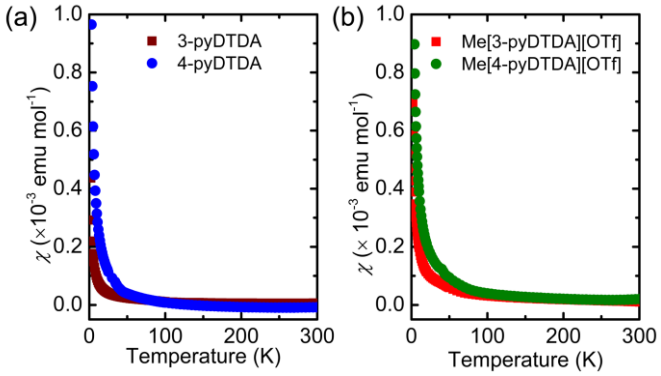

Figure 11. Cooling curve plots of χ versus T for (a) 3-, 4-pyDTDA and (b) Me[3-, 4-pyDTDA][OTf] over the range 2-300 K at a field H = 0.1 T.

Summary and Conclusions

The chemistry and structural properties of DTDA and DSDA radicals have been extensively studied for many years. A wide range of 4-substituents have been explored, with increasing interest in the introduction of ligands that can enhance or complement the coordination chemistry of the radical itself.[21,23,24] In principle a 3- or 4-pyridyl ligand provides an effective secondary binding site for metal ions, but the basic nature of these ligands also introduces subtleties in the preparation of the radicals to which they are bound. Here we have provided a detailed account of the preparation of 3-, 4-pyDTDA and their Se-based analogues, using procedures that reflect the intermediacy of protonated radicals. Treatment of the protonated intermediates with base allows for isolation and structural characterization of the native radicals. In the solid state 3, 4-pyDTDA and 3, 4-pyDSDA crystallize as diamagnetic dimers linked head-to-tail into ribbon-like arrays by short η^2-S_2---N(py) and η^2-Se_2---N(py) intermolecular secondary bonding interactions. In the case of 4-pyDTDA disorder in the packing of these molecular ribbons leads to a nanocrystalline morphology.

As a first step in exploiting the basic properties of the 3-, 4-pyridyl ligands we have prepared the *N*-methylated radical triflates Me[3-, 4-pyDTDA][OTf], the crystal structures of which consist of diamagnetic *trans*-cofacial dimers strongly ion-paired with triflate anions. Development of the charge transfer chemistry of these latter salts opens the door to the development of new functional molecular materials with potentially interesting magnetic and/or charge transport properties.

Experimental Section

General Methods and Procedures. The starting materials 3- and 4-cyanopyridine, benzyltriethylammonium chloride, lithium bis(trimethylsilylamide), chlorotrimethylsilane, methyl trifluoromethanesulfonate (methyl triflate), silver trifluoromethanesulfonate (silver triflate), sulfur monochloride, potassium iodide, and triphenylantimony were obtained commercially; all were used as received, save for KI, which was dried in vacuo. Selenium tetrachloride was prepared following the literature procedure.[33] Reagent grade acetonitrile (MeCN) was dried by distillation from P_2O_5 and CaH_2, anhydrous grade tetrahydrofuran (THF) was dried by distillation from sodium/benzophenone and diethyl ether was dried over 4 Å molecular sieves. Unless otherwise specified, all reactions and synthetic procedures were carried out under an atmosphere of nitrogen or argon. Fractional sublimations of all radical dimers were performed in an ATS series 3210 three-zone tube furnace, mounted horizontally and linked to a series 1400 temperature control system. Infrared spectra (Nujol mulls, KBr optics) were recorded on a Nicolet Avatar FTIR spectrometer or Bruker Alpha with Platinum ATR module with a diamond IR transmitting crystal at 2 cm^{-1} resolution. NMR spectra were recorded on a Bruker Avance III HD 300 MHz spectrometer using anhydrous deuterated solvents. Elemental analyses

were performed in-house on an Elementar Vario EL III elemental analyzer or by MHW Laboratories, Phoenix, AZ 85018.

Preparation of (*E*)-*N*,*N*,*N*'-Tris(trimethylsilyl)isonicotinimidamide, 4-pyADS. Solid lithium bis(trimethylsilyl)amide (26.0 g, 0.156 mol) was added to a solution of 4-cyanopyridine (10.4 g, 0.100 mol) in 75 mL THF. The mixture was heated at reflux for 4 h, cooled to room temperature and chlorotrimethylsilane (15.0 mL, 0.118 mol) added to afford an off-white precipitate. The mixture was heated for an additional 16 h, then filtered and the solvent removed in vacuo to leave an oil that was purified by vacuum distillation at 110 °C/10^{-1} Torr; yield 18.0 g (53.5 mmol, 54%). The distilled oil crystallized on cooling, and the resulting material could be recrystallized from either MeCN or hexane as colorless needles, mp 45-46 °C. ^{1}H NMR (δ, $CDCl_3$): 8.55 (d, 1H, Ar-H, J = 5.71 Hz), 7.13 (d, 1H, Ar-H, J = 5.61 Hz), 0.05 (s, 9H, -$Si(CH_3)_3$).[34] IR (nujol mull): 1633 (s), 1590 (m), 1548 (w), 1247 (s), 1131 (w), 997 (w), 840 (s), 757 (w) cm^{-1}. Anal. Calcd for $C_{15}H_{31}N_3Si_3$: C, 53.35; H, 9.25; N, 12.44. Found: C, 53.15; H, 9.12; N, 12.63.

Preparation of 4-(Pyridin-4-yl)-1,2,3,5-dithiadiazolyl, 4-pyDTDA. Sulfur monochloride (18.5 g, 0.138 mmol) was added to a solution of 4-pyADS (2.40 g, 8.30 mmol) in 50 mL anhydrous MeCN. The mixture was heated at reflux for 2 h, cooled to room temperature, and the light purple precipitate of the double salt [4-pyDTDA][Cl][HCl] was filtered off, washed with 3 × 20 mL MeCN and dried in vacuo, yield 2.04 g (8.04 mmol). IR (nujol mull, Figure 2a): 1631 (s), 1597 (s), 1544 (s), 1507 (m), 1483 (w), 1307 (s), 1230 (m), 1193 (w), 1115 (vs), 1076 (w), 894 (w), 817 (m), 772 (m), 629 (s), 529 (m) cm^{-1}. This crude material was added to 50 mL MeCN, along with solid Ph_3Sb (3.81 g, 9.94 mmol) and $[BzEt_3N][Cl]$ (2.14 g, 38 mmol). The resulting slurry was stirred at room temperature for 1 h, and the dark purple precipitate of the

crude radical hydrochloride [4-pyDTDA][HCl] filtered off, washed with 3 × 20 mL MeCN and dried in vacuo, yield 1.67 g (7.65 mmol). IR (nujol mull, Figure 2b): 1632 (s), 1609 (s), 1522 (m), 1507 (m), 1370 (s), 1247 (m), 1189 (w), 1150 (s), 1088 (m), 1088 (w), 1001(m), 979 (w), 835 (s), 817 (s), 778 (s), 724 (m), 644 (m), 514 (m) cm^{-1}. Finally, deprotonation of the crude [4-pyDTDA][HCl] was effected by treating a slurry of it (1.42 g, 6.47 mmol) in 40 mL MeCN with NEt_3 (1.45 g, 14.3 mmol) for 30 min. The purple powder of crude 4-pyDTDA so produced was filtered off, washed with 3 × 20 mL MeCN and dried in vacuo; yield 1.10 g (6.03 mmol, 93% from [4-pyDTDA][HCl]). Black microcrystalline nodules of 4-pyDTDA suitable for chemical analysis and magnetic measurements were obtained by vacuum sublimation of the crude material at 10^{-4} Torr in a three-zone tube furnace along a temperature gradient of 50 - 100 °C; dec > 150 °C. IR (nujol mull, Figures 2c and S1): 1597 (m), 1417 (s), 1138 (w), 1061 (w), 998 (w), 826 (s), 808 (m), 785 (s), 655 (m), 511 (m) cm^{-1}. Anal. Calcd for $C_6H_4N_3S_2$: C, 39.54; H, 2.21; N, 23.06. Found: C, 39.56; H, 2.33; N, 23.19.

Preparation of (*E*)-*N*,*N*,*N*'-Tris(trimethylsilyl)nicotinimidamide, 3-pyADS. Solid lithium bis(trimethylsilyl)amide (18.0 g, 0.108 mol) was added to a solution of 3-cyanopyridine (10.4 g, 0.100 mol) in 75 mL anhydrous THF. The reaction was heated at reflux for 4 h, then cooled to room temperature and chlorotrimethylsilane (15.0 mL, 0.118 mol) added to afford an off-white precipitate. The reaction was heated at reflux for an additional 16 h, after which time the precipitate was filtered off and the solvent removed in vacuo to leave 3-pyADS as an oil that was purified by vacuum distillation at 110 °C/10^{-1} Torr; yield 18.4 g (0.544 mol, 54%). ^{1}H NMR (δ, $CDCl_3$): 8.52 (d, 1H, Ar-H, J = 3.84 Hz), 8.49 (s, 1H, Ar-H), 7.51 (m, 1H, Ar-H), 7.19 (m, 1H, Ar-H), 0.02 (s, 9H, -Si(CH_3)$_3$). Anal. Calcd for $C_{15}H_{31}N_3Si_3$: C, 53.35; H, 9.25; N, 12.44. Found: C, 53.40; H, 9.28; N, 12.22.

Preparation of 4-(Pyridin-3-yl)-1,2,3,5-dithiadiazolyl, 3-pyDTDA. Following the procedure described above for 4-pyDTDA, sulfur monochloride (13.5 g, 0.100 mol) was added to a solution of 3-pyADS (1.70 g, 5.04 mmol) in 50 mL MeCN. The resulting slurry was heated at reflux for 2 h, then cooled to room temperature, and the orange precipitate of the crude double salt solid [3-pyDTDA][Cl][HCl] was filtered off, washed with 3 × 20 mL MeCN and dried in vacuo, yield 1.21 g (4.74 mmol). This crude material was added to 50 mL MeCN, along with solid Ph_3Sb (1.71 g, 4.84 mmol) and $[BzEt_3N][Cl]$ (1.33 g, 5.83 mmol). The resulting slurry was stirred at room temperature for 1 h, and the dark purple precipitate of the crude radical hydrochloride [3-pyDTDA][HCl] filtered off, washed with 3 × 20 mL MeCN and dried in vacuo, yield 0.936 g (4.28 mmol). Deprotonation of the crude [3-pyDTDA][HCl] with NEt_3 (1.09 g, 10.8 mmol) in 25 mL MeCN for 30 min afforded crude 3-pyDTDA, which was filtered off, washed with 3 × 20 mL MeCN and dried in vacuo; yield 0.689 g (3.78 mmol, 88% from [3-pyDTDA][HCl]). Analytically pure crystals of 3-pyDTDA suitable for crystallographic work and magnetic measurements were obtained by vacuum sublimation of the crude product at 10^{-4} Torr in a three-zone tube furnace along a temperature gradient of 50 - 100 °C afforded a lustrous dark blue crystalline solid; dec > 150 °C. IR (nujol mull, Figure S1): 1587 (w), 1187 (w), 1146 (m), 1040 (w), 1024 (m), 832 (m), 807 (s), 781 (s), 699 (s), 667 (m), 627 (w), 512 (m) cm^{-1}. Anal. Calcd for $C_6H_4N_3S_2$: C, 39.54; H, 2.21; N, 23.06. Found: C, 39.36; H, 2.32; N, 23.17.

Preparation of Methyl-(*E*)-*N*,*N*,*N*'-tris(trimethylsilyl)nicotinimidamide Triflate, Me[3-pyADS][OTf]. A solution of 3-pyADS (4.17 g, 12.3 mmol) in 35 mL of Et_2O was cooled on an ice/water bath while neat methyl triflate (1.60 mL, 13.87 mmol) was added dropwise over 5 min. The reaction was allowed to warm to room temperature and stirred for 16 h to afford a yellow solution. The solvent was flash distilled to leave a white solid, which was washed with 20 mL

toluene and the fine white solid collected by filtration and dried in vacuo; yield 5.66 g (11.28 mmol, 91 %). ^{1}H NMR (δ, CD_3CN): 9.11 (s, 1H, Ar-H), 8.74 (d, 1H, Ar-H, *J* = 9 Hz), 8.65 (d, 1H, Ar-H, *J* = 3 Hz), 8.04 (dd, 1H, Ar-H, *J* = 3 and 9 Hz), 4.33 (s, 3H, N-Me), 0.02-0.07 (s, br, 27H, -Si(CH_3)$_3$). This material was used for subsequent reactions without further purification.

Preparation of Me[3-pyDTDA][OTf]$_2$. Neat sulfur monochloride (7.93 g, 58.7 mmol) was added dropwise to a solution of Me[3-pyADS][OTf] (7.42 g, 14.8 mmol) in 60 mL MeCN to afford an orange solution. The mixture was stirred at room temperature for 16 h, then solid [$BzEt_3N$][Cl] (6.74 g, 29.6 mmol) was added to afford a heavy orange precipitate of Me[3-pyDTDA][Cl]$_2$. After stirring for 1 h the crude solid was filtered off, washed with 3 × 40 mL MeCN and dried in vacuo. To a slurry of this crude Me[3-pyDTDA][Cl]$_2$ in 50 ml MeCN was added an excess TMSOTf (12.0 mL, 66.3 mmol) to afford a clear light blue solution over a white solid. The mixture was stirred at room temperature for 1 h, then filtered and the volatiles were removed from the filtrate by flash distillation to afford a beige solid which was recrystallized from 20 mL of MeCN at -20 ^{o}C as colorless blocks of Me[3-pyDTDA][OTf]$_2$ which were collected by filtration and dried in vacuo; yield 12.0 g (24.3 mmol, 84 %). IR (ATR): 3352 (br, m), 3151 (br, m), 3077 (m), 1705 (m), 1645 (m), 1595 (w), 1486 (m), 1412 (m), 1342 (vw), 1257 (s), 1239 (s), 1218 (vs), 1151 (vs), 1017 (vs), 918 (m), 865 (m), 834 (sh, m), 791 (vs), 760 (w), 721 (w), 675 (w), 629 (s), 573 (m), 558 (m), 513 (s), 463 (w), 407 (vw) cm^{-1}. ^{1}H NMR (δ, CD_3CN): 9.23 (s, 1H, Ar-H), 8.47 (d, 1H, Ar-H, *J* = 7 Hz), 8.71 (d, 1H, Ar-H, *J* = 6 Hz), 8.14 (dd, 1H, Ar-H, *J* = 6 and 7 Hz) 4.38 (s, 3H, N-Me). Anal. Calcd for $C_9H_7N_3O_6F_6S_4$: C, 21.82; H, 1.42; N, 8.48. Found: C, 22.81; H, 1.66; N, 8.70.

Preparation of Me[3-pyDTDA][OTf]. A mixture of KI (2.25 g, 13.6 mmol) and Me[3-pyDTDA][OTf]$_2$ (3.03 g, 6.12 mmol) in 70 mL MeCN was stirred at room temperature for 90

min to afford a lustrous bronze precipitate of Me[3-pyDTDA][I] which was collected by filtration and washed with 5 × 20 mL MeCN, 10 mL DCM and then dried in vacuo; yield 1.13 g (3.49 mmol, 57 %). IR (ATR): 3062 (m), 3012 (m), 2957 (vw), 2936 (w), 1811 (vw), 1775 (w), 1638 (m), 1591 (w), 1504 (m), 1475 (m), 1400 (w), 1378 (m), 1325 (w), 1288 (w), 1256 (m),1210 (s), 1187 (w), 1139 (s), 1123 (s), 1031 (s), 957 (w), 909 (vw), 813 (vs), 774 (vs), 657 (vs), 651 (m), 618 (m), 539 (vw), 511 (s), 486 (s), 446 (m), 408 (m). A small excess of AgOTf (0.666 g, 2.59 mmol) was added to a suspension of Me[3-pyDTDA][I] (0.832 g, 2.57 mmol) in 40 mL of MeCN and the mixture stirred for 1 h at room temperature to afford a dark orange solution over a pale yellow precipitate of AgI. The supernatant solution was drawn off with a cannula and concentrated in vacuo to ca. 5 mL. Cooling the solution to -20 ^{o}C for 24 h afforded lustrous orange blocks of Me[3-pyDTDA][OTf] that were collected by filtration, washed with 2 × 15 mL of DCM and dried in vacuo; yield 0.344 g (0.993 mmol, 38 %). IR (ATR): 3076 (w), 3049 (w), 1703 (w), 1642 (w), 1592 (vw), 1479 (w), 1409 (m), 1257 (vs), 1237 (vs), 1218 (vs), 1201 (vs), 981 (vs), 916 (w), 864 (m), 816 (w), 787 (w), 757 (w), 688 (m), 675 (w), 629 (s), 574 (m), 513 (m), 460 (s), 424 (w). Anal. Calcd for $C_8H_7F_3N_3S_3O_3$: C, 27.74; H, 2.04; N, 12.13. Found: C, 27.52; H, 2.10; N, 12.30.

Preparation of Methyl-(*E*)-*N*,*N*,*N*'-tris(trimethylsilyl)isonicotinimidamide Triflate, Me[4-pyADS][OTf]. A solution of 4-pyADS (3.45 g, 10.2 mmol) in 30 mL diethyl ether (Et_2O) was cooled on an ice/water bath while methyl triflate (1.10 mL, 10.0 mmol) in 10 mL of Et_2O was added dropwise over 5 min. The reaction was allowed to warm temperature and stirred at 5 ^{o}C for 16 h, then the fine white precipitate of Me[4-pyADS][OTf] was collected by filtration, washed with 2 × 20 mL Et_2O and dried in vacuo; yield 4.54 g (9.04 mmol, 88 %). ^{1}H NMR (δ, CD_3CN): 8.64 (d, 1H, Ar-H, J = 6 Hz), 8.281 (s, br, 1H, Ar-H), 8.11 (s, br, 1H, Ar-H), 4.30 (s,

3H, N-Me), 0.30 (s, 9H, -Si(CH_3)$_3$), 0.06 (s, 18H, -Si(CH_3)$_3$). This material was used for subsequent reactions without further purification.

Preparation of Me[4-pyDTDA][OTf]$_2$. Neat sulfur monochloride (9.28 g, 68.8 mmol) was added dropwise to a solution of Me[4-pyADS][OTf] (5.75 g, 11.5 mmol) in 60 mL MeCN to afford a red-orange solution. The mixture was stirred at room temperature for 16 h, then solid [$BzEt_3N$][Cl] (5.86 g, 25.7 mmol) was added to afford an orange precipitate. After stirring for 1 h the bright orange precipitate of Me[4-pyDTDA][Cl]$_2$ was filtered off, washed with 3 × 40 mL MeCN and dried in vacuo. To a slurry of this crude Me[4-pyDTDA][Cl]$_2$ in 60 mL MeCN was added an excess of TMSOTf (8.00 mL, 30.8 mmol) to afford a straw yellow solution which was stirred at room temperature for 1 h. The solution was filtered and the volatiles were removed from the filtrate by flash distillation to afford a beige solid which was recrystallized from 25 mL MeCN at -20 ^oC to afford pale yellow blocks of Me[4-pyDTDA][OTf]$_2$ which were collected by filtration and dried in vacuo; yield 4.57 g (3.81 mmol, 81 %). IR (ATR): 3342 (br, m), 3127 (br, w), 3064 (m), 3026 (w), 1692 (m), 1648 (m), 1584 (w), 1522 (vw), 1485 (m), 1468 (w), 1437 (m), 1398 (w), 1235 (br, vs), 1221 (s), 1165 (s), 1152 (vs), 1105 (s), 1056 (w), 1026 (vs), 997 (m), 905 (w), 871 (w), 856 (m), 844(w), 799 (m), 758 (s), 719 (s), 689 (s), 632 (vs), 573 (m), 554 (w), 516 (s), 495 (w), 442 (m) cm^{-1}. ^1H NMR (δ, CD_3CN): 8.72 (d, 2H, Ar-H, J = 6 Hz), 8.37 (d, 2H, Ar-H, J = 6 Hz), (s, 1H, Ar-H), 4.31 (s, 3H, N-Me). Anal. Calcd for $C_9H_7N_3O_6F_6S_4$: C, 21.82; H, 1.42; N, 8.48. Found: C, 22.13; H, 1.52; N, 8.77.

Preparation of Me[4-pyDTDA][OTf]. A mixture of KI (0.452 g, 2.72 mmol) and Me[4-pyDTDA][OTf]$_2$ (0.632 g, 1.28 mmol) in 20 mL MeCN was stirred at room temperature for 2 h to afford a lustrous bronze precipitate of Me[4-pyDTDA][I] which was collected by filtration, washed with 5 × 15 mL of MeCN, 15 mL DCM and dried in vacuo; yield 0.296 g (0.913 mmol,

72 %). IR (ATR): 3109 (m), 3087 (w), 3035 (m), 3016 (m), 2978 (m), 1693 (vs), 1634 (w), 1585 (w), 1566 (w), 1519 (s), 1469 (vs), 1404 (s), 1367 (w), 1325 (s), 1291 (m), 1257 (s), 1205 (s), 1177 (w), 1144 (vs), 1066 (vs), 1045 (m), 1031 (m), 978 (w), 966 (w), 912 (w), 845 (m), 816 (m), 795 (m), 770 (s), 726 (w), 666 (w), 640 (m), 617 (m), 598 (vw), 511 (m), 485 (m), 440 (m). A small excess of AgOTf (0.479 g, 1.864 mmol) was added to a suspension of Me[4-pyDTDA][I] (0.294 g, 0.907 mmol) in 25 mL of MeCN and the mixture stirred for 4 h at room temperature to afford a dark orange solution over a pale yellow precipitate of AgI. The supernatant solution was drawn off using a cannula and concentrated in vacuo to ca. 5 mL. Cooling the solution -20 ^{o}C for 24 h afforded lustrous orange plates of Me[4-pyDTDA][OTf] that were collected by filtration, washed with 2 × 15 mL of DCM and dried in vacuo; yield 0.095 g (0.274 mmol, 30 %). IR (ATR): 3132 (w), 3072 (w), 1641 (m), 1583 (w), 1466 (m), 1426 (w), 1396 (m), 1274 (vs), 1253 (vs), 1219 (vs), 1203 (vs), 1147 (vs), 1051 (w), 1020 (vs), 948 (w), 916 (m), 857 (m), 758 (w), 741 (w), 681 (w), 667 (vw), 630 (vs), 573 (s), 553 (m), 516 (vs) 456 (w). Anal. Calcd for $C_8H_7F_3N_3S_3O_3$: C, 27.74; H, 2.04; N, 12.13. Found: C, 27.65; H, 2.15; N, 12.16.

Preparation of 4-(3′-pyridyl)-1,2,3,5-diselenadiazolyl, 3-pyDSDA. A solution of 3-pyADS (1.00 g, 2.96 mmol**)** in 10 mL MeCN was added to a solution of $SeCl_2$ prepared in situ from selenium powder (0.234 g, 2.96 mmol) and $SeCl_4$ (0.654 mg, 2.96 mmol) in 50 mL MeCN to afford an red-brown precipitate. The mixture was stirred at room temperature for 1 h, then the crude [3-pyDSDA][Cl] was filtered off, washed with 3 × 15 mL MeCN and dried in vacuo; crude yield 0.860 g (2.76 mmol, 93%). IR: 1678 (m), 1585 (w), 1187 (w), 1137 (w), 1039 (w), 1023 (w), 870 (w), 810 (w), 706 (m) cm^{-1}. Powdered triphenylantimony (1.20 g, 3.40 mmol) was then added to a slurry of the crude [3-pyDSDA][Cl] (0.860 g, 2.76 mmol) in 20 mL MeCN and

the mixture stirred at room temperature for 16 h. The resulting black precipitate of crude 3-pyDSDA was filtered off, washed with 3 × 15 mL MeCN and dried in vacuo; crude yield 0.754 g (2.73 mmol, 99 %). Crystals suitable for crystallographic work were obtained by vacuum sublimation at 10^{-4} Torr in a three-zone furnace along a temperature gradient of 60 - 140 °C; dec > 150 °C; IR (nujol mull, Figure S1): 1584 (m), 1420 (s), 1320 (s), 1197 (m), 1129 (m), 1040 (m), 1026 (m), 809 (w), 714 (s), 637 (m) cm^{-1}. Anal. Calcd for $C_6H_4N_3Se_2$: C, 26.11; H, 1.46; N, 15.22. Found: C, 26.18; H, 1.61; N, 15.40.

Preparation of 4-(4′-pyridyl)-1,2,3,5-diselenadiazolyl, 4-pyDSDA. A solution of 4-pyADS (1.22 g, 3.61 mmol) in 10 mL MeCN was added to a solution of $SeCl_2$ prepared in situ from selenium powder (0.235 g, 3.60 mmol) and $SeCl_4$ (0.797 g, 3.61 mmol) in 50 mL MeCN to afford a red-brown precipitate. The mixture was stirred at room temperature for 1 h, then the crude [4-pyDSDA][Cl] was filtered off, washed with 3 × 15 mL MeCN and dried in vacuo; yield 0.976 g (3.13 mmol, 87%). Powdered triphenylantimony (1.51 g, 4.23 mmol) was added to a slurry of crude [4-pyDSDA][Cl] (0.976 g, 3.13 mmol) in 20 mL of degassed MeCN and the mixture stirred at room temperature for 16 h. The resulting black precipitate of crude 4-pyDSDA was filtered off, washed with 3 × 15 mL MeCN and dried in vacuo; crude yield 0.840 g (3.04 mmol, 97%). Crystals suitable for crystallographic work were obtained by vacuum sublimation at 10^{-4} Torr in a three-zone furnace along a temperature gradient of 60 - 140 °C; dec > 150 °C; IR (nujol mull, Figure S1): 1593 (m), 1412 (m), 1323 (w), 1204 (w), 1064 (w), 998 (m), 830 (m), 727 (m), 707 (w), 660 (m) cm^{-1}. Anal. Calcd for $C_6H_4N_3Se_2$: C, 26.11; H, 1.46; N, 15.22. Found: C, 26.24; H, 1.50; N, 15.20.

EPR Spectroscopy. X-Band EPR spectra for 3- and 4-pyDTDA were recorded at ambient temperature using a Bruker EMX-200 or Magnettech high resolution MS200 spectrometer;

sublimed samples of the radicals were dissolved in degassed DCM, while the cation-radicals were dissolved in MeCN and transferred under Argon atmosphere into a quartz flat cell. Hyperfine coupling constants were obtained by spectral simulation using Simfonia and WinSim.[35]

Single Crystal Crystallography. Crystals of 3-pyDTDA, Me[3-, 4-pyDTDA][OTf]$_2$ and Me[3-, 4-PyDTDA][OTf] were coated with Fomblin oil and mounted on a MiTeGen loop, while those of [3-, 4-PyDSDA] were mounted on glass fibers with epoxy. X-ray data for 3-pyDTDA were collected at 296 K on beamline I19 at the Diamond Light Source (λ = 0.68890 Å) using Rigaku CrystalClear[36] and processed with Bruker APEX2[37] software and SADABS.[38] X-ray data for Me[3-, 4-pyDTDA][OTf]$_2$ and Me[3-, 4-PyDTDA][OTf] were collected at 120 K on an Agilent SupraNova diffractometer equipped with multilayer optics monochromated dual source (Cu and Mo) and Atlas detector, using CuK$_\alpha$ (λ = 1.54184 Å) radiation; data acquisitions, reductions and analytical face-index based absorption corrections were made using the program CrysAlisPRO.[39] For 3-, 4-PyDSDA X-ray data were collected at 296 K using ω scans with a Bruker APEX II CCD detector on a D8 three-circle goniometer and Mo Kα (λ = 0.71073 Å) radiation. In all cases, the structures were solved using the ShelXS[40] program and refined on F^2 by full matrix least squares techniques with the ShelXL8 program using the interface in the Olex2 (v.1.2) program package.[41]

Powder Crystallography. Powdered samples of sublimed 4-pyDTDA were loaded into borosilicate glass capillaries and sealed. Data were collected at 293 K using synchrotron radiation (λ = 0.825925 Å) available on beamline I11 at the Diamond Light Source. As a result of the paucity and poor resolution of some of the observed reflections attempts to index the data using DICVOL,[42] McMaille[43] and Topas[44] were unsuccessful. However, starting from the cell

settings and space group (*C*2/*c*) of 4-pyDSDA manual indexing of the data was eventually achieved. A structure search was then performed in DASH[45] using simulated annealing methods and a molecular unit based on the atomic coordinates of 4-cyanophenyl-DTDA.[15] A rigid body constraint was initially employed, followed by release of the ring-to-ring (py-DTDA) torsion angle. A solution was found which closely matched the *cis*-cofacial mode of dimerization and packing observed in 4-pyDSDA (Figures 3 and 6). The occurrence of two other simulated annealing solutions with the same cell parameters and similar profile χ^2 values but comprised of ribbons of *trans*-cofacial and *trans*-antarafacial dimers (Figures S6 and S7) points to a disordered nanocrystalline phase[30] in which there is a large number of faults in the layering of the molecular ribbons. This would explain the poor crystalline growth (powdery nodules) of 4-pyDTDA compared to 4-pyDSDA and the low resolution and broad peaks observed in the PXRD diffractogram. While we prefer the *cis*-cofacial structure, by virtue of its similarity to 4-pyDSDA, all three solutions were individually refined by Rietveld methods[46] using the GSAS program,[47] with atomic positions and isotropic thermal parameters taken from the initial DASH refinement. Atomic positions were not further refined and, as a result, standard deviations for atomic coordinates are not available. Final Rietveld indices R_p and R_{wp} for all three models are listed in Table S2. The deposited CIF file for 4-pyDTDA corresponds to the *cis*-cofacial dimer; for completenesss the refined crystal coordinates for the other two models are available in Tables S4 and S5.

Magnetic Susceptibility Measurements. DC magnetic susceptibility measurements were performed at a field of 1000 Oe over the temperature range 2-300 K on a Quantum Design MPMS SQUID magnetometer. Diamagnetic corrections were made using Pascal's constants.[48]

Corresponding Authors

aaronmailman@gmail.com; oakley@uwaterloo.ca

Notes. The authors declare no competing financial interest.

Acknowledgement. This work was supported by the Natural Sciences and Engineering Research Council of Canada (NSERCC), the University of Jyväskylä, the Academy of Finland (projects 253907 and 289172), the European Union's H2020 research and innovations programme (under the Marie Skłodowska-Curie Grant Agreement 659123), CNRS, the University of Bordeaux, the Région Nouvelle Aquitaine, the GdR MCM-2 and the MOLSPIN COST action CA15128. We thank the Diamond Light Source for access to beamlines I11 and I19.

References and Notes

[1] (a) Oakley, R. T. Cyclic and Heterocyclic Thiazenes. *Prog. Inorg. Chem.* **1988**, *36*, 299. (b) Banister, A. J.; Rawson, J. M. Some Synthetic and Structural Aspects of Dithiadiazoles, RCN_2S_2, and Related Compounds. In *The Chemistry of Inorganic Ring Systems*, ed. R. Steudel, Elsevier, Amsterdam, 1992, p. 323. (c) Cordes, A. W.; Haddon, R. C.; Oakley, R. T. Heterocyclic Thiazyl and Selenazyl Radicals; Synthesis and Applications in Solid State Architecture. In *The Chemistry of Inorganic Ring Systems*, ed. R. Steudel, Elsevier, Amsterdam, 1992, p. 295. (d) Rawson, J. M.; Banister, A. J.; Lavender, I. The Chemistry of Dithiadiazolylium and Dithiadiazolyl Rings. *Adv. Heterocycl. Chem*. **1995**, *62*, 137. (e) Haynes, D. A. Crystal engineering with dithiadiazolyl radicals. *CrystEngComm* **2011**, *13*, 4793.

[2] (a) Rawson, J. M.; Luzon, J.; Palacio, F. Magnetic exchange interactions in perfluorophenyl dithiadiazolyl radicals. *Coord. Chem. Rev*. **2005**, *249*, 2631. (b) Rawson, J. M.; Alberola, A.; Whalley, A. Thiazyl radicals: old materials for new molecular devices. *J. Mater. Chem*. **2006**, *16*, 2560.

[3] (a) Oakley, R. T. Chemical Binding within and between Inorganic Rings; the Design and Synthesis of Molecular Conductors. *Can. J. Chem*. **1993**, *71*, 1775. (b) Bryan, C. D.; Cordes, A. W.; Fleming, R. M.; George, N. A.; Glarum, S. H.; Haddon, R. C.; MacKinnon, C. D.; Oakley, R. T.; Palstra, T. T. M.; Perel, A. S. Charge Transfer Salts of Benzene-bridged 1,2,3,5-Dithiadiazolyl Diradicals; Preparation, Structures and Transport Properties of 1,3- and 1,4-$[(S_2N_2C)C_6H_4(CN_2S_2)][X]$ (X = I, Br). *J. Am. Chem. Soc*. **1995**, *117*, 6880. (c) Bryan, C. D.; Cordes, A. W.; Goddard, J. D.; Haddon, R. C.; Hicks, R. G.; MacKinnon, C. D.; Mawhinney, R. C.; Oakley, R. T.; Palstra, T. T. M.; Perel, A. S. Preparation and Characterization of the Disjoint Diradical 4,4′-Bis(1,2,3,5-dithiadiazolyl) $[S_2N_2C\text{-}CN_2S_2]$ and its Iodine Charge Transfer Salt $[S_2N_2C\text{-}CN_2S_2][I]$. *J. Am. Chem. Soc.* **1996**, *118*, 330.

[4] (a) Preuss, K. E. Metal complexes of thiazyl radicals. *Dalton Trans*. **2007**, 2357. (b) Preuss, K. E. Metal-radical coordination complexes of thiazyl and selenazyl ligands. *Coord. Chem. Rev*. **2015**, *289*, 45. (c) Lau, H. F.; Ang, P. C. Y.; Ng, V. W. L.; Kuan, S. L.; Goh, L. Y.; Borisov, A. S.; Hazendonk, P.; Roemmele, T. L.; Boeré, R. T.; Webster, R. D. Coupling of $CpCr(CO)_3$ Heterocyclic Dithiadiazolyl Radicals. Synthetic, X-ray Diffraction, Dynamic NMR, EPR, CV and DFT Studies. *Inorg. Chem*. **2008**, *47*, 632. (d) Lau, H. F.; Ng, V. W. L.; Koh, L. L.; Tan, G. K.; Goh, L. Y.; Roemmele, T. L.; Seagrave, S.; Boeré, R. T. Cyclopentadienylchromium complexes of 1,2,3,5-dithiadiazolyls: η^2 π-complexes of cyclic sulphur-nitrogen compounds. *Angew. Chem., Int. Ed*. **2006**, *45*, 4498.

[5] (a) Beldjoudi, Y.; Osorio-Román, I.; Nascimento, M. A.; Rawson, J. M. A fluorescent dithiadiazolyl radical: structure and optical properties of phenanthrenyl dithiadiazolyl in solution and polymer composites. *J. Mater. Chem. C* **2017**, *5*, 2794. (b) Beldjoudi, Y.; Nascimento, M. A.; Cho, Y. J.; Yu, H.; Aziz, H.; Tonouchi, D.; Eguchi, K.; Matsushita, M. M.; Awaga, K.; Osorio-Roman, I.; Constantinides, C. P.; Rawson, J. M. Multifunctional Dithiadiazolyl Radicals: Fluorescence, Electroluminescence, and Photoconducting Behavior in Pyren-1′-yl-dithiadiazolyl. *J. Am. Chem. Soc*. **2018**, *140*, 6260.

[6] Matsui, H.; Yamane, M.; Tonami, T.; Nagami, T.; Watanabe, K.; Kishi, R.; Kitagawa, Y.; Nakano, M. Theoretical study on the gigantic effect of external static electric field application on the nonlinear optical properties of 1,2,3,5-dithiadiazolyl π-radical dimers. *Mater. Chem. Front.* **2018**, *2*, 785.

[7] Potts, S. V.; Barbour, L. J.; Haynes, D. A.; Rawson, J. M.; Lloyd, G. O. Inclusion of Thiazyl Radicals in Porous Crystalline Materials. *J. Am. Chem. Soc.* **2011**, *133*, 12948.

[8] Nikolayenko, V. I.; Barbour, L. J.; Arauzo, A.; Campo, J.; Rawson, J. M.; Haynes, D. A. Inclusion of a dithiadiazolyl radical in a seemingly non-porous solid. *Chem. Commun*. **2017**, *53*, 11310.

[9] Banister, A. J.; Bricklebank, N.; Clegg, W.; Elsegood, M. R. J.; Gregory, C. I.; Lavender I.; Rawson, J. M.; Tanner, B. K. The first solid state paramagnetic 1,2,3,5-dithiadiazolyl radical; X-ray crystal structure of [*p*-NCC_6F_4CNSSN]·. *J. Chem. Soc., Chem. Commun*. **1995**, 679.

[10] Boeré, R. T.; Hill, N. D. D. High *Z′* structures of 1,2,3,5-dithiadiazolyls and of 1,2,3,5-diselenadiazolyls containing the first structurally characterized monomeric diselenadiazolyls. *CrystEngComm*, **2017**, *19*, 3698.

[11] Gleiter, R.; Haberhauer, G. Electron-rich two-, three- and four-center bonds between chalcogens - New prospects for old molecules. *Coord Chem. Rev*. **2017**, *344*, 263.

[12] (a) Beekman, R. A.; Boeré, R. T.; Moock, K. H.; Parvez. M. Synthesis, electrochemistry, structure and magnetic susceptibility of 5-*tert*-butyl-1,3-bis-(1,2,3,5-dithiadiazolyl)benzene. Structural effects of the bulky substituent. *Can. J. Chem.* **1998**, *76*, 85. (b) Melen, R. L.; Less, R. J.; Pask, C. M.; Rawson, J. M. Structural Studies of Perfluoroaryldiselenadiazolyl Radicals: Insights into Dithiadiazolyl Chemistry. *Inorg. Chem*. **2016**, *55*, 11747.

[13] (a) Beneberu, H. Z.; Tian, Y. H.; Kertesz, M. Bonds or not bonds? Pancake bonding in 1,2,3,5-dithiadiazolyl and 1,2,3,5-diselenadiazolyl radical dimers and their derivatives. *Phys. Chem. Chem. Phys.* **2012**, *14*, 10713. (b) Tian, Y. H.; Kertesz, M. Is There a Lower Limit to the CC Bonding Distances in Neutral Radical π-Dimers? The Case of Phenalenyl Derivatives *J. Am. Chem. Soc*. **2010**, *132*, 10648. (c) Mou, Z.; Tian, Y-H.; Kertesz, M. Validation of density functionals for pancake-bonded π-dimers; dispersion is not enough. *Phys. Chem. Chem. Phys*. **2017**, *19*, 24761. (d) Preuss, K. E. Pancake bonds: π-Stacked dimers of organic and light-atom radicals. *Polyhedron* **2014**, *79*, 1. (e) Kertesz, M. Pancake bonding, an unusual pi-stacking interaction. *Chem. Euro. J.* **2018**, doi.org/10.1002/chem.201802385.

[14] (a) Andrews, M. P.; Cordes, A. W.; Douglass, D. C.; Fleming, R. M.; Glarum, S. H.; Haddon, R. C.; Marsh, P.; Oakley, R. T.; Palstra, T.T.M.; Schneemeyer, L. F.; Trucks, G. W.; Tycko, R. W.; Waszczak, J. V.; Warren, W. W.; Young, K. M.; Zimmerman, N. M. One-Dimensional Stacking of Bifunctional Dithia- and Diselenadiazolyl Radicals; Preparation, Structural and Electronic Properties of 1,3-[(E_2N_2C)C_6H_4(CN_2E_2)] (E = S, Se). *J. Am. Chem. Soc.* **1991**, *113*, 3559. (b) Cordes, A. W.; Haddon, R. C.; Hicks, R. G.; Oakley, R. T.; Palstra, T. T. M.; Schneemeyer, L. F.; Waszczak, J. V. Polymorphism of 1,3-Phenylene Bis(diselenadiazolyl); Solid State Structural and Electronic Properties of *β*-1,3-[(Se_2N_2C)C_6H_4(CN_2Se_2)]. *J. Am. Chem. Soc.* **1992**, *114*, 1729.

[15] Cordes, A. W.; Haddon, R. C.; Hicks, R. G.; Oakley, R. T.; Palstra, T. T. M. Preparation and Solid State Structures of Cyanophenyl Dithia- and Diselenadiazolyl Radicals. *Inorg. Chem*. **1992**, *31*, 1802.

[16] Cordes, A. W.; Chamchoumis, C. M.; Hicks, R. G.; Oakley, R. T.; Young, K. M.; Haddon, R. C. Mono- and Difunctional Furan-based 1,2,3,5-Dithiadiazolyl Radicals; Preparation and Solid State Structures of 2,5-[(S_2N_2C)OC_4H_2(CN_2S_2)] and 2,5-[(S_2N_2C)OC_4H_2(CN)]. *Can. J. Chem*. **1992**, *70*, 919.

[17] Britten, J. F.; Clements, O. P.; Cordes, A. W.; Haddon, R. C.; Oakley, R. T.; Richardson, J. F. Stacking Efficiency of Diselenadiazolyl *π*-Dimers. Consequences for Electronic Structure and Transport Properties. *Inorg. Chem*. **2001**, *40*, 6820.

[18] (a) Clarke, C. S.; Haynes, D. A; Smith, J. N. B.; Batsanov, A. S.; Howard, J. A. K.; Pascu, S. I.; Rawson, J. M. The effect of fluorinated aryl substituents on the crystal structures of 1,2,3,5-dithiadiazolyl radicals. *CrystEngComm* **2010**, *12*, 172. (b) Beldjoudi, Y.; Arauzo, A.; Palacio, F.; Pilkington, M.; Rawson, J. M. Studies on a "Disappearing Polymorph": Thermal and Magnetic Characterization of *α*-*p*-NCC_6F_4CNSSN. *J. Am. Chem. Soc.* **2016**, *138*, 16779.

[19] (a) Banister, A. J.; Bricklebank, N.; Lavender, I.; Rawson, J. M.; Gregory, C. I.; Tanner, B. K.; Clegg, W.; Elsegood, M. R. J.; Palacio, F. Spontaneous magnetization in a sulfur-nitrogen radical at 36 K. *Angew. Chem., Int. Ed. Engl.* **1996**, *35*, 2533. (b) Thomson, R. I.; Pask, C. M.; Lloyd, G. O.; Mito, M.; Rawson, J. M. Pressure-Induced Enhancement of Magnetic-Ordering Temperature in an Organic Radical to 70 K: A Magnetostructural Correlation. *Chem. Eur. J.*

2012, *18*, 8629. (c) Deumal, M.; Rawson, J. M.; Goeta, A. E.; Howard, J. A. K.; Copley, R. C. B.; Robb, M. A.; Novoa, J. J. Studying the Origin of the Antiferromagnetic to Spin-Canting Transition in the beta-*p*-$NCC_6F_4CNSSN\cdot$ Molecular Magnet. *Chem. Eur. J.* **2010**, *16*, 2741. (d) Alberola, A.; Less, R. J.; Pask, C. M.; Rawson, J. M.; Palacio, F.; Oliete, P.; Paulsen, C.; Yamaguchi, A.; Farley, R. D.; Murphy, D. M. A thiazyl-based organic ferromagnet *Angew. Chem., Int. Ed.* **2003**, *42*, 4782.

[20] Constantinides, C. P.; Carter, E.; Eisler, D.; Beldjoudi, Y.; Murphy, D. M.; Rawson, J. M. Effects of Halo-Substitution on 2′-Chloro-5′-halo-phenyl-1,2,3,5-dithiadiazolyl Radicals: A Crystallographic, Magnetic, and Electron Paramagnetic Resonance Case Study. *Cryst. Growth Des.* **2017**, *17*, 3017.

[21] (a) Hearns, N. G.; Preuss, K. E.; Richardson, J. F.; Bin-Salamon, S. Design and Synthesis of a 4-(2′-Pyridyl)-1,2,3,5-Dithiadiazolyl Cobalt Complex. *J. Am. Chem. Soc.* **2004**, *126*, 9942. (b) Jennings, M.; Preuss, K. E.; Wu, J. Synthesis and magnetic properties of a 4-(2′-pyrimidyl)-1,2,3,5-dithiadiazolyl dimanganese complex. *Chem. Commun*. **2006**, 341. (c) Britten, J.; Hearns, N. G.; Preuss, K. E.; Richardson, J. F.; Bin-Salamon, S. Mn(II) and Cu(II) Complexes of a Dithiadiazolyl Radical Ligand: Monomer/Dimer Equilibria in Solution. *Inorg. Chem*. **2007**, *46*, 3934. (d) Hearns, N. G.; Fatila, E. M.; Clérac, R.; Jennings, M.; Preuss, K. E. Ni(II) and hs-Fe(II) complexes of a paramagnetic thiazyl ligand, and decomposition products of the iron complex, including an Fe(III) tetramer. *Inorg. Chem.* **2008**, *47*, 10330. (e) Hearns, N. G.; Clérac, R.; Jennings, M.; Preuss, K. E. Manipulating the crystal packing of pyDTDA radical ligand coordination complexes with Mn(II) and Ni(II). *Dalton Trans.* **2009**, 3193. (f) Fatila, E. M.; Goodreid, J.; Clérac, R.; Jennings, M.; Assoud, J.; Preuss, K. E. High-spin supramolecular pair of Mn(II)/thiazyl radical complexes. *Chem. Commun*. **2010**, *46*, 6569. (g) Wu, J.; MacDonald, D. J.; Clérac, R.; Jeon, I.-R.; Jennings, M.; Lough, A. J.; Britten, J.; Robertson, C.; Dube, P. A.; Preuss, K. E. Metal complexes of bridging neutral radical ligands: pymDTDA and pymDSDA. *Inorg. Chem*. **2012**, *51*, 3827. (h) Fatila, E. M.; Mayo, R. A.; Rouzières, M.; Jennings, M. C.; Dechambenoit, P.; Soldatov, D. V.; Mathonière, C.; Clérac, R.; Coulon, C.; Preuss, K. E. Radical-Radical Recognition: Switchable Magnetic Properties and Re-entrant Behavior. *Chem. Mater*. **2015**, *27*, 4023. (i) Fatila, E. M.; Maahs, A. C.; Mills, M. B.; Rouzières, M.; Soldatov, D.

V.; Clérac, R.; Preuss, K. E. Ferromagnetic ordering of -[Sm(III)-radical]$_n$- coordination polymers. *Chem. Commun*. **2016**, *52*, 5414.

[22] The proper names for these radicals are 4-(3′-pyridyl)- and 4-(4′-pyridyl)-1,2,3,5-dithiadiazolyl. For convenience we use the abbreviations 3-pyDTDA and 4-pyDTDA throughout this paper.

[23] Wong, W.-K.; Sun, C.; Wong, W.-Y.; Kwong, D. W. J.; Wong, W.-T. Synthesis and Chemistry of Dithiadiazole Free Radicals [4-(4′-C_5H_4N)CN_2S_2] and [4-(3′-C_5H_4N)CN_2S_2]; X-ray Crystal Structures of [Pd_3{μ-SNC(Ar′)NS-*S*,*S*′}$_2$(PPh_3)$_4$] (Ar′ = 4′-C_5H_4N, 4′-$C_5H_4NBEt_3$ and 3′-$C_5H_4NBEt_3$). *Eur. J. Inorg. Chem*. **2000**, 1045.

[24] Haynes, D. A.; van Laeren, L. J.; Munro, O. Q. Cobalt Porphyrin-Thiazyl Radical Coordination Polymers: Toward Metal-Organic Electronics. *J. Am. Chem. Soc*. **2017**, *139*, 14620.

[25] (a) Alange, G. G.; Banister, A.J.; Bell, B.; Millen, P. W. 1,2,3,5-Dithiadiazolium Chlorides, [RCN_2S_2]Cl. *Inorg. Nucl. Chem. Lett*. **1977**, *13*, 143. (b) Alange, G. G.; Banister, A. J.; Bell, B.; Millen, P. W. Preparation of some 1,2,3,5-dithiadiazolium chlorides from trichlorocyclotrithiazene and nitriles or olefins, and from amidinium salts and sulfur dichloride. *J. Chem. Soc., Perkin Trans. I* **1979**, 1192. (c) Höfs, H.-U.; Mews, R.; Clegg, W.; Noltemeyer, M.; Schmidt, M.; Sheldrick, G. M. 4-Chloro-1,2,3,5-dithiadiazolium salts. *Chem. Ber*. **1983**, *116*, 416.

[26] Cordes, A. W.; Haddon, R. C.; Hicks, R. G.; Kennepohl, D. K.; Oakley, R. T.; Schneemeyer, L. F.; Waszczak, J. V. Preparation and Solid State Structure of 1,3,5-Triazine-2,4,6-tris-(1,2,3,5-dithiadiazolyl). *Inorg. Chem*. **1993**, *32*, 1554.

[27] Boeré, R. T.; Oakley, R. T.; Reed, R. W. Preparation of *N*,*N*,*N*'-Tris(trimethysilyl)amidines; a Convenient Route to Unsubstituted Amidines. *J. Organomet. Chem*. **1987**, *331*, 161. (b) Boeré, R. T.; Hicks, R. G.; Oakley, R. T. *N*,*N*,*N*'-Tris(trimethylsilyl)amidines. *Inorg. Synth*. **1997**, *31*, 94.

[28] (a) Del Bel Belluz, P.; Cordes, A. W.; Kristof, E. M.; Kristof, P.; Liblong, S. W.; Oakley, R. T. 1,2,3,5-Diselenodiazolyls as Building Blocks for Molecular Metals; Preparation and Structures

of $[PhCN_2Se_2]^+$ PF_6^- and $[PhCN_2Se_2]_2$. *J. Am. Chem. Soc*. **1989**, *111*, 9276. (b) Cordes, A. W.; Bryan, C. D.; Davis, W. M.; de Laat, R. H.; Glarum, S. H.; Goddard, J. D.; Haddon, R. C.; Hicks, R. G.; Kennepohl, D. K.; Oakley, R. T.; Scott, S. R.; Westwood, N. P. C. Prototypal 1,2,3,5-Dithia- and Diselenadiazolyl $[HCN_2E_2]\cdot$ (E = S, Se); Molecular and Electronic Structures of the Radicals and their Dimers, by Theory and Experiment. *J. Am. Chem. Soc*. **1993**, *115*, 7232.

[29] Robinson, S. W.; Haynes, D. A.; Rawson, J. M. Co-crystal formation with 1,2,3,5-dithiadiazolyl radicals. *CrystEngComm* **2013**, *15*, 10205.

[30] (a) Gorelik, T. E.; Czech, C.; Hammer, S. M.; Schmidt, M. U. Crystal structure of disordered nanocrystalline α^{II}-quinacridone determined by electron diffraction. *CrystEngComm* **2016**, *18*, 529. (b) Lincke, G.; Finzel, H.-U. Studies on the Structure of alpha-Quinacridone. *Cryst. Res. Technol.* **1996**, *31*, 441. (b) Lekin, K.; Leitch, A. A.; Assoud, A.; Yong, W.; Desmarais, J.; Tse, J. S.; Desgreniers, S.; Secco, R. A.; Oakley, R. T. Benzoquinone-Bridged Heterocyclic Zwitterions as Building Blocks for Molecular Semiconductors and Metals. *Inorg. Chem*. **2018**, *57*, 4757.

[31] Domagała, S.; Haynes, D. A. Experimental and theoretical charge density assessments for the 4-perfluoropyridyl- and 4-perflurophenyl-1,2,3,5-dithiadiazolyl radicals. *CrystEngComm* **2016**, *18*, 7116.

[32] Fairhurst, S. A.; Johnson, K. M.; Sutcliffe, L. H.; Preston, K. F.; Banister, A. J.; Hauptman, Z. V.; Passmore, J. Electron spin resonance study of $CH_3CNSSN\cdot$, $C_6H_5CNSSN\cdot$, and $SNSSN\cdot^+$ free radicals. *J. Chem. Soc., Dalton Trans.* **1986**, 1465.

[33] Brauer, G. Handbook of Preparative Chemistry; Academic: New York, 1963; Vol. 1, p 423.

[34] Banerjee, A.; Ngwendson, J. N. US patent 20070179311 A1 (2007).

[35] WinEPR Simfonia, version 1.25; Bruker Instruments, Inc.: Billerica, MA, 1996.

[36] *CrystalClear*; Rigaku Corporation: Tokyo, Japan, 2005.

[37] *APEX2*; Bruker AXS Inc.: Madison, WI, 2007.

[38] *SADABS*; Bruker AXS Inc.: Madison, WI, 2001.

[39] Agilent CrysalisPro, Agilent Technologies Ltd., Yarnton, England, 2010.

[40] Sheldrick, G. M. SHELXT - Integrated space-group and crystal-structure determination. *Acta Crystallogr. A* **2008**, *64*, 112.

[41] Dolomanov, O. V.; Bourhis, L. J.; Gildea, R. J.; Howard, J. A. K.; Puschmann, H. J. OLEX2: A Complete Structure Solution, Refinement and Analysis Program. *J. Appl. Cryst.* **2009**, *42*, 339.

[42] Boultif, A.; Louer, D. Powder Pattern Indexing with the Dichotomy Method. *J. Appl. Crystallogr*. **2004**, *37*, 724.

[43] Le Bail, A. Monte Carlo indexing with McMaille. *Powder Diffraction* **2004**, *19*, 249.

[44] Coelho, A. A. TOPAS and TOPAS-Academic: an optimization program integrating computer algebra and crystallographic objects written in C++. *J. Appl. Cryst.* **2018**, *51*, 210.

[45] David, W. I. F.; Shankland, K.; van de Streek, J.; Pidcock, E.; Motherwell, W. D. S.; Cole, J. C. DASH: a Program for Crystal Structure Determination from Powder Diffraction Data. *J. Appl. Crystallogr*. **2006**, *39*, 910.

[46] Rietveld, H. M. A Profile Refinement Method for Nuclear and Magnetic Structures. *J. Appl. Crystallogr*. **1969**, *2*, 65.

[47] Larson, A. C.; Von Dreele, R. B. General Structure Analysis System (GSAS); Los Alamos National Laboratory Report LAUR 86-748; 2000.

[48] (a) Carlin, R. L. Magnetochemistry; Springer-Verlag: New York, 1986. (b) Bain, G. A.; Berry, J. F. Diamagnetic Corrections and Pascal's Constants. *J. Chem. Educ.* **2008**, *85*, 532.